Temperature Distribution in Tubular Solid Oxide Fuel Cell

Kiyoshi KANAMURA,* Shoji YOSHIOKA, and Zen-ichiro TAKEHARA
Department of Industrial Chemistry, Faculty of Engineering, Kyoto University, Yoshida-Honmachi, Sakyo-ku, Kyoto 606
(Received February 7, 1991)

The temperature distribution in the tubular solid oxide fuel cell (SOFC) was calculated by using a finite element method. In this study, specially, the heat generation and consumption caused by the entropy changes at anode and cathode were taken into account for the calculation of temperature distribution in SOFC. In order to estimate the tendency of temperature distribution, the current distribution and the partial pressure distributions of hydrogen, steam, and oxygen were obtained from the calculation by using the simple mathematical model. From the temperature distribution in the tubular SOFC, it can be seen that the temperature difference is largest in the region of porous cathode material. This indicates that the heat generation from the entropy change of cathode reaction has the significant effect for the temperature distribution in tubular solid oxide fuel cell.

Solid oxide fuel cell (SOFC) has been investigated and developed, because of the high energy conversion efficiency. These researches have been concentrated on the development of the electrode materials, the electrolyte materials, and the construction of the cell.[1] Recently the excellent design of SOFC has been achieved by using Electrochemical Vapor Deposition (EVD).[2] The thin electrolyte was deposited on the conductive oxide cathode which was deposited on the porous calcia stabilized zirconia. The tubular SOFC is suitable for EVD process. In this study, the temperature distribution in the tubular SOFC was calculated by a finite element method in order to offer the fundamental knowledge for the development of the high energy conversion SOFC.

The maximum electric energy generated in SOFC corresponds to ΔG of the hydrogen combustion which is the total reaction in SOFC when oxygen and hydrogen are used. ΔH of this reaction, however, is the total energy which can be utilized in SOFC. The energy of $T\Delta S$ cannot be utilized as an electric energy. Since SOFC is operated at high temperature (around 1273 K), the energy of $T\Delta S$ is lost as a heat which amount is much larger than those from other fuel cells operated at low temperature (around 450 K). Moreover, the energy loss is also caused by both overpotentials of hydrogen and oxygen electrodes and the ohmic loss of the electrolyte. These irreversible factors generate the heat in SOFC. In order to minimize the energy loss caused by the overpotential and ohmic resistance, the thickness of electrolyte has to be decreased and the excellent oxygen and hydrogen electrodes have to be developed. The energy loss caused by the entropy change, however, can not be improved, because of the thermodynamic limiting. From this fact, it can be concluded that the temperature distribution caused by the heat generated or consumed by the entropy change of electrode reactions is more important.

The heat management of SOFC is the most important problem for the construction of the SOFC and the determination of the practical operating conditions. Therefore, the calculation of the temperature distribution was conducted by using a finite element method.

Experimental

Yttria stabilized zirconia was prepared by the sintering of the mixture of Y_2O_3 8 mol% and ZrO_2 92 mol% (Toyo Soda Corp.). Its oxygen ion conductance was measured by using AC impedance method at 1273 K. The entropy changes at oxygen and hydrogen electrodes were determined by the measurement of Seebeck coefficients according to the reference.[3]

The temperature distribution in the tubular SOFC was calculated by using the program for a finite element method.[4] From our calculation, the tendency of the temperature distribution can be obtained. The electrochemical parameters of oxygen and hydrogen electrodes reported in reference[5] were used for the estimation of heat generated from oxygen and hydrogen overpotentials. For the simple calculation, some assumptions were adopted.

Results and Discussion

Heat Generation Factors. The heat is generated by the irreversible processes taking place in SOFC and thermodynamic factors in an electrochemical system. In SOFC, the heat is generated or absorbed by the following factors;

(1) Overpotentials of hydrogen and oxygen electrodes.

(2) Ohmic resistance of yttria stabilized zirconia.

(3) Entropy changes at hydrogen and oxygen electrodes.

The overpotentials of hydrogen and oxygen electrodes are dependent on the current. The relationships between the overpotentials and the current for oxygen and hydrogen electrodes have been examined and suggested by many researchers.[5–7] The electrochemical parameters depend on the kind of electrode. In this study, the model cell is constructed by $LaCoO_3$ as a cathode, Ni cermet as an anode, yttria stabilized zirconia as an electrolyte and porous yttria stabilized zirconia as a support. The following equations were adopted in the calculation of the heat generation caused by the

Table 1. Electrochemical Parameters Used in the Calculation of the Current Distribution

Electrochemical parameters	
I_0	9.8 A m^{-2}
K	0.0609 V[a)]
σ[b)]	0.1 S cm^{-1}

a) $K=RT/4\alpha F$ from Ref. 5, α: transfer coefficient, R: gas constant, F: Faraday constant. b) $R=(1/\sigma)(L/S)$; L: thickness of YSZ of element, S: surface area of YSZ of element.

overpotentials in order to simplify the calculation. Table 1 shows the electrochemical parameters which have been suggested in the reference.[5)]

For hydrogen electrode

$$\eta_a = K \ln\left(\frac{I}{I_0}\right) \tag{1}$$

For oxygen electrode

$$\eta_c = 0 \tag{2}$$

where η_a and η_c are overpotentials of anode and cathode, respectively, I_0 is exchange current, I is current, and K is the constant listed in Table 1. The heat generation from the ohmic resistance of yttria stabilized zirconia is also dependent on the current. The relationship between the voltage loss in the electrolyte (ΔV) and the current (I) obeys Ohm's law.

$$\Delta V = IR \tag{3}$$

where R is the resistance of the electrolyte in the tubular SOFC, which is estimated from the conductivity of yttria stabilized zirconia (YSZ). The conductivity of YSZ can be measured by using the impedance method.[8)]

The heat generation caused by the entropy change becomes larger with increasing temperature. The heat caused by the entropy changes at hydrogen and oxygen electrodes has to be taken into account for the calculation of the temperature distribution. The total reaction in SOFC is the hydrogen combustion. The total entropy change (ΔS) is easily estimated from the thermodynamic consideration. The total reaction, however, is separated to cathode and anode reactions in an electrochemical cell. The entropy change is also separated to cathode and anode reactions. In other words, an entropy change of single electrode ($\Delta S_{cathode}$ for the entropy change of cathode reaction, ΔS_{anode} for the entropy change of anode reaction) have to be estimated.

$$\Delta S = \Delta S_{cathode} + \Delta S_{anode} \tag{4}$$

The entropy changes of cathode and anode can be estimated from Seebeck coefficients of oxygen and hydrogen electrodes, as reported in reference.[3)] The entropy change of oxygen electrode reaction was estimated to be -81.6 J K^{-1} mol^{-1} per two electrons under 0.21×10^5 Pa oxygen partial pressure at 1273 K. From Eq. 4, the entropy change of hydrogen electrode can be calculated. These values are dependent on the partial pressure. The dependence can be represented by the following equations.

Total reaction

$$H_2 + \frac{1}{2}O_2 \rightarrow H_2O \tag{5}$$

For hydrogen electrode,

$$\Delta S_{anode} = (S_{H_2O} - R\int_1^{P_{H_2O}} d\ln P) - (S_{H_2} - R\int_1^{P_{H_2}} d\ln P) - S_{O^{2-}}{}^* \tag{6}$$

For oxygen electrode,

$$\Delta S_{cathode} = S_{O^{2-}}{}^* - \frac{1}{2}(S_{O_2} - R\int_1^{P_{H_2O}} d\ln P) \tag{7}$$

where $S_{O^{2-}}{}^*$ is the transported entropy of O^{2-} ion in yttria stabilized zirconia. The entropy changes of hydrogen and oxygen electrodes under various partial pressures can be calculated from Eqs. 6 and 7. $\Delta S_{cathode}$ changes with the partial pressure of oxygen and ΔS_{anode} changes with the partial pressures of hydrogen and steam in SOFC. Therefore, the partial pressure distribution has to be estimated in order to calculate the temperature distribution in the tubular SOFC. The entropy change of single electrode reaction is represented by the function of temperature. In this study, however, it was assumed that the dependence of entropy change on temperature in narrow temperature region was too small to influence the temperature distribution.

Calculation of Current and Partial Pressure Distributions. The current and partial pressure distribution in solid oxide fuel cell have been reported in some references.[9,10)] In this study, the current distribution was calculated by using the model, as shown in Fig. 1. This is the typical tubular SOFC which has metal oxide

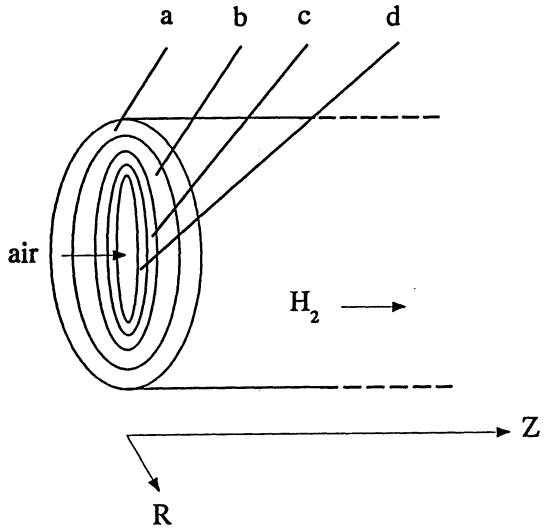

Fig. 1. Schematic illustration of tubular SOFC constructed by electrolyte (yttria stabilized zirconia), anode (Ni zirconia cermet electrode), cathode ($LaCoO_3$), and porous zirconia substrate.

cathode, Ni–ZrO_2 cermet anode, yttria stabilized zirconia electrolyte, and porous yttria stabilized zirconia support. Hydrogen is flown through the outside of cell and oxygen through the inside of cell. The dimension of the cell is summarized in Table 2. In order to calculate the current distribution in this SOFC, the cell is divided to n elements, as shown in Fig. 2. The simple mathematical procedure was used for the calculation of the current and partial pressure distributions in the tubular SOFC. The equivalent circuit for this model is shown in Fig. 3. The current passed through each element is represented by I_i. R_i indicates the resistance of yttria stabilized zirconia electrolyte in i th element. Z_i is the sum of both impedances of oxygen and hydrogen electrodes. The total current (I) is given by the sum of each elementary current (I_i).

$$I = I_1 + I_2 + \cdots + I_i + \cdots + I_n \tag{8}$$

If both electrodes have high electric conductivity, the cell voltage of each element is equal to the cell voltage (V).

$$V = V_1 = V_2 = \cdots = V_i = \cdots = V_n \tag{9}$$

Table 2. Dimension of the Tubular SOFC

Length (L)	20 cm
Diameter inside	10 mm
outside (D)	17 mm
Thickness of cathode	0.5 mm
Thickness of anode	0.5 mm
Thickness of electrolyte	0.5 mm
Thickness of porous substrate	2 mm

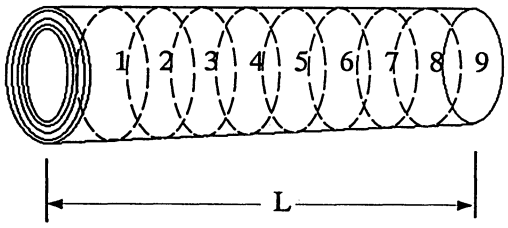

Fig. 2. Model for calculation of current and partial pressure distribution.

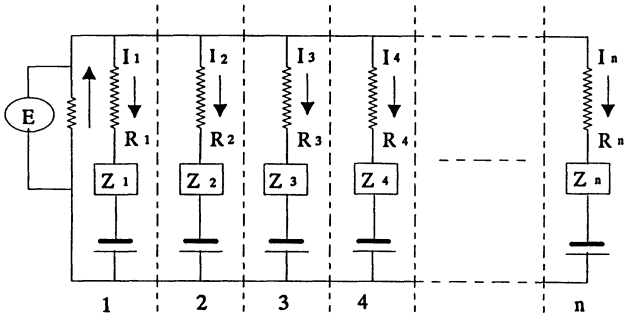

Fig. 3. Equivalent circuit for the model in Fig.2.

For element 1, the relationship between V_1 and I_1 is represented by the following equation,

$$V_1 = E_e - \eta_1 - R_1 I_1 \tag{10}$$

where η_1 is the total overpotential of element 1 and is given by the Eqs. 1, 2, and 11. η_i is given by the sum of both overpotentials of hydrogen and oxygen electrodes.

$$\eta_i = \eta_{ia} + \eta_{ic} \tag{11}$$

where η_{ia} and η_{ic} are the overpotential of hydrogen electrode of element i and that of oxygen electrode of element i, respectively. E_e is the equilibrium voltage of solid oxide fuel cell and is determined from the partial pressures of hydrogen, steam, and oxygen according to Nernst equation.

$$E_e = E_0 - (RT/2F)\ln(P_{H_2O}/P_{O_2}^{1/2} P_{H_2}) \tag{12}$$

For the other elements, the same relationship can be established. The hydrogen and oxygen flow horizontally through the chambers in the cell at constant rate. The partial pressures of oxygen and hydrogen at the entrance of chamber are higher than those at the exit, because oxygen and hydrogen are consumed by the electrode reactions at each element. The partial pressure of steam at the entrance of fuel chamber is lower than that at the exit. The hydrogen partial pressure in element 2 is given by the following equation,

$$P_{H_2,2} = \frac{U_{H_2,1} - \dfrac{I_1}{2F}}{\left(U_{H_2,1} - \dfrac{I_1}{2F}\right) + \left(U_{H_2O,1} + \dfrac{I_1}{2F}\right)} \tag{13}$$

The air and steam partial pressures are given by the similar equations.

$$P_{air,2} = \frac{0.21\,U_{air,1} - \dfrac{I_1}{4F}}{U_{air,1} - \dfrac{I_1}{4F}} \tag{14}$$

$$P_{H_2O,2} = \frac{U_{H_2O,1} + \dfrac{I_1}{2F}}{\left(U_{H_2O,1} + \dfrac{I_1}{2F}\right) + \left(U_{H_2,1} - \dfrac{I_1}{2F}\right)} \tag{15}$$

where $U_{i,1}$ is the flow rate of gas i at the entrance of SOFC (mol s^{-1}). In this way, the partial pressure in element 2 can be obtained. As a result, E_e can be also determined. The elementary current in element 2, I_2, can be calculated from E_e and V by using Eq. 10. Such a procedure is repeated n times. Finally, the current distribution and the partial pressure distribution can be calculated.

Figure 4 shows the equilibrium voltage and the total overpotential distributions along Z-axis in the tubular SOFC calculated from above simple mathematical model, where the total current and gas flow rate are

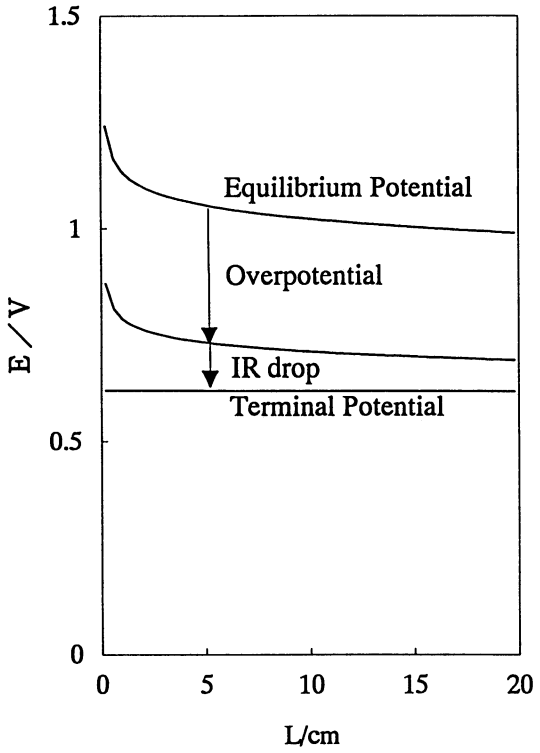

Fig. 4. Distributions of the equilibrium potential and IR drop in the tubular SOFC, discharge current: 200 mA cm^{-2}, flow rate: 5 cm s^{-1}.

assumed to be 200 mA cm^{-2} and 5 cm s^{-1}, respectively. The utilization of hydrogen depends on the flow rate. The flow rate was assumed to be 5 cm s^{-1}, in order to obtain the fuel utilization to be about 10%. These distributions result in the current distribution in the tubular SOFC.

Figure 5 shows the current distribution in SOFC at two flow rates of hydrogen. The average current density is 200 mA cm^{-2}. The partial current near the entrance of SOFC is larger than that near the exit according to the potential distribution in Fig. 4. The current distribution depends on the flow rate and become larger with decreasing of the flow rate. The heat generation caused by the ohmic resistance of electrolyte is seemed to be much larger at the entrance of cell compared with the heat generation at the exit, as expected from the relationship between the heat generation at the electrolyte and the current.

Figure 6 shows the partial pressure distributions of oxygen, hydrogen, and steam in SOFC at 5 cm s^{-1} (0.0376 mol s^{-1}) flow rate. The hydrogen partial pressure gradually decreases along the Z axis from the entrance to the exit. Under these conditions, 10% of hydrogen induced in SOFC is consumed by the electrode reaction. The oxygen partial pressure also decreases. The partial pressure distribution of hydrogen is larger than that of oxygen, because 4 electron per 1 mole oxygen is consumed at the oxygen electrode and 2 electron per 1 mole hydrogen is consumed at the

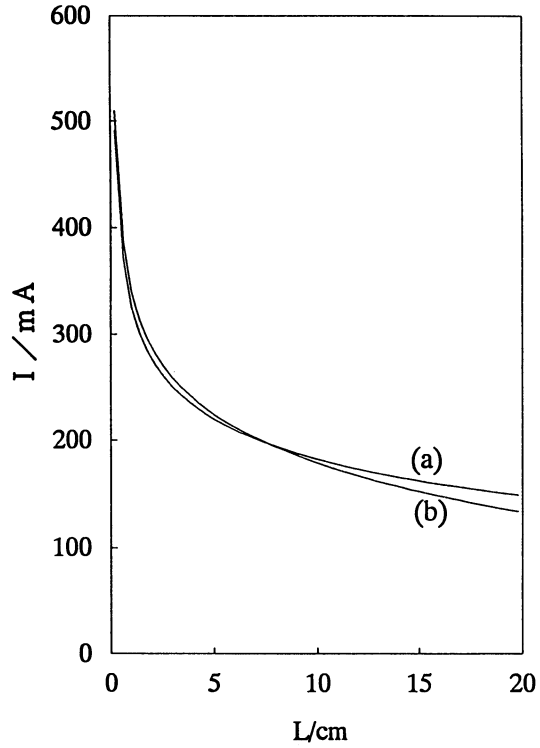

Fig. 5. Current distribution in the tubular SOFC, discharge current: 200 mA cm^{-2}, flow rate: 5 cm s^{-1} (a) and 20 cm s^{-1} (b).

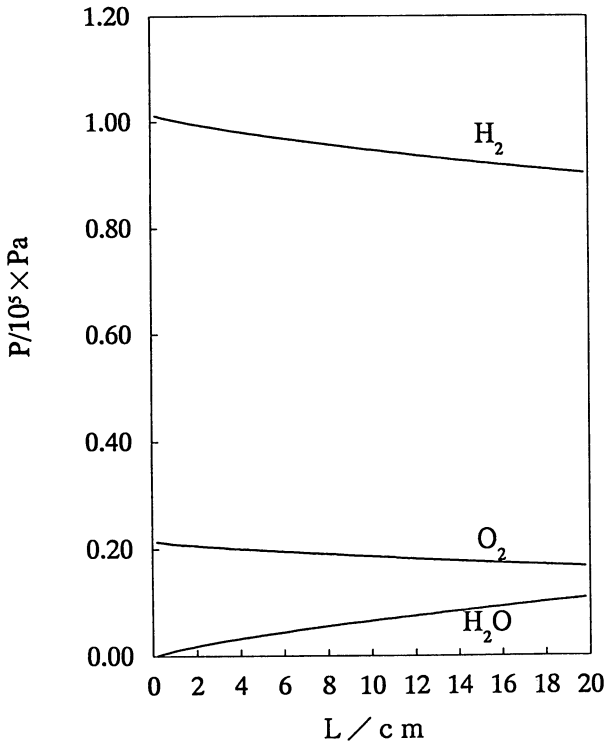

Fig. 6. Partial pressure distributions in the tubular SOFC, discharge current; 200 mA cm^{-2}, flow rate; 5 cm s^{-1}.

hydrogen electrode. The partial pressure distributions of hydrogen and steam are larger than that of oxygen. The heat caused by the entropy change of oxygen and hydrogen electrodes can be estimated from the partial pressure distributions of gasses according to Eqs. 13, 14, and 15.

In this way, the partial pressure distributions of hydrogen, oxygen, and steam and the current distribution in SOFC were obtained. From these results, the heat generation at each element can be estimated. The temperature distribution in SOFC can be calculated by using a finite element method.

Temperature Distribution in Tubular SOFC. Figure 7 shows the model of the tubular SOFC and the initial and boundary conditions for the calculation of a finite element method. The gas temperature was assumed to be 1273 K to simplify the calculation. The temperature distribution at steady state was estimated in this study. The heat conductivities of yttria stabilized zirconia, porous yttria stabilized zirconia support, $LaCoO_3$, and Ni cermet are summarized in Table 3. At the interface between the oxygen chamber and the porous yttria stabilized zirconia, the thermal boundary is assumed. The heat transfer coefficients of the thermal boundary between air and yttria stabilized zirconia support (h_{in}) can be written by

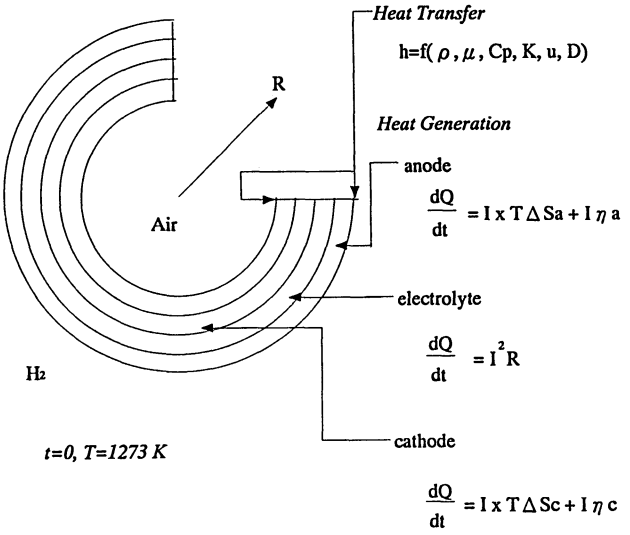

Fig. 7. Model for calculation of temperature distribution and initial and boundary conditions.

Table 3. Heat Conductivities of the Materials in SOFC

Material	κ/J cm^{-1} s^{-1} K^{-1}
YSZ	0.027
Porous YSZ	0.011
$LaCoO_3$	0.022
Ni cermet	0.11

Table 4. Physical Parameters of Hydrogen and Air at 1273 K

	ρ/g cm^{-3}	μ/g cm^{-1} s^{-1}	C_p/J g^{-1} K^{-1}	κ/J cm^{-1} s^{-1} K^{-1}
Air	0.276	6×10^{-5}	1.1×10^{3}	0.2
H_2	0.019	3×10^{-5}	1.4×10^{4}	0.1

$$h_{in} = Nu\ \kappa / D \tag{16}$$

where Nu (Nusselt constant) is calculated from physicochemical properties of air by using the following equations.

$$Nu = 2.43\ (Re\ Pr\ D/L)^{1/3} \tag{17}$$

$$Pr = C_p\ \mu / \kappa \tag{18}$$

$$Re = Du\ \rho / \mu \tag{19}$$

ρ is the density of gas, μ the viscosity of gas, C_p the heat capacity of gas, κ the heat conductivity, u the flow rate of gas, D the diameter of the cell, L the length of the cell, Pr Prandtl constant, and Re Reynolds number. These parameters are summarized in Table 2 and 4. On the other hand, the heat transfer coefficient of thermal boundary between hydrogen chamber and anode (h_{out}) can be given by the following equation

$$h_{out} = 0.664\ (\kappa / L)\ Re^{1/2}\ Pr^{1/3} \tag{20}$$

In this way, the heat transfer coefficients at the interfaces are easily calculated from these equations. The heat generation at oxygen electrode can be estimated by

$$\frac{dQ}{dt} = IT\Delta S_c + I\eta_c \tag{21}$$

and at hydrogen electrode

$$\frac{dQ}{dt} = IT\Delta S_a + I\eta_a \tag{22}$$

The heat generation from electrolyte is given by

$$\frac{dQ}{dt} = I^2R \tag{23}$$

The hydrogen and oxygen flows along Z-axis from the entrance to the exit. The hydrogen electrode is made from nickel cermet and its thickness is 500 μm. The oxygen electrode is made from $LaCoO_3$ and its thickness is 500 μm. The electrolyte is the yttria stabilized zirconia and its thickness is 500 μm. The thickness of each element is related to the mechanical strength of the cell. The thick element gives the high reliability of the cell. In this study, the thickness of each element was assumed from the point of view of the stability of the cell.

Thus, all parameters used in the calculation of the temperature distribution in the tubular SOFC can be estimated. The calculation by using a finite element method was carried out. Figure 8 shows the temperature distribution in the electrolyte along Z-axis. The temperature at the entrance is lower than that at the exit. From the current distribution, it is expected that the heat energy generated at the entrance is larger than

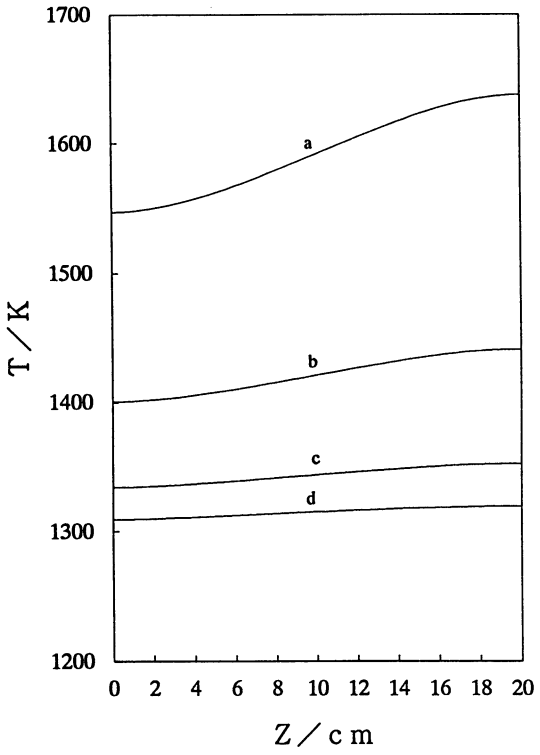

Fig. 8. Temperature distribution in YSZ along Z-axis at a: 5 cm s^{-1}, b: 10 cm s^{-1}, c: 20 cm s^{-1}, and d: 30 cm s^{-1}.

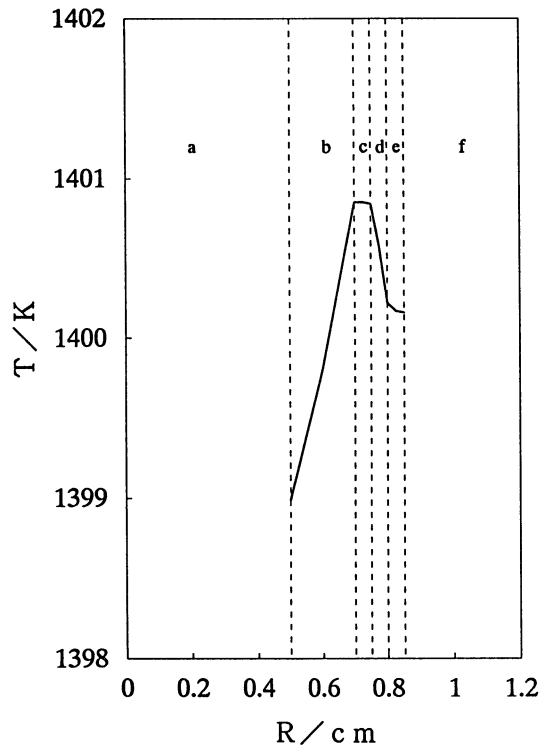

Fig. 9. Temperature distribution along R-axis near the entrance of the tubular SOFC at 10 cm s^{-1}, a: air chamber, b: porous substrate, c: cathode, d: electrolyte, e: anode, f: fuel chamber.

that at the exit. The temperature distribution in Fig. 8, however, is inconsistent with such an expectation. This fact indicates that the heat generated near the entrance of SOFC is transported to hydrogen gas and oxygen gas. At the exit of the tubular SOFC, the heat is transported form hydrogen gas and oxygen gas to the electrolyte during the initial period of the discharge. Therefore the temperature in electrolyte near the exit is higher than that at the entrance. The temperature distribution in SOFC strongly depends on the flow rate. The uniform temperature distribution can be obtained at 30 cm s^{-1} flow rate. The utilization of fuel, however, decreased with increasing of flow rate.

Figure 9 shows the temperature distribution along R-axis near the entrance of SOFC. The highest temperature is observed at the electrolyte region. The temperatures at porous yttria stabilized zirconia and the nickel cermet electrode are lower than that at the electrolyte. The heat is transported from the electrolyte to hydrogen and oxygen gasses. The temperature gradient is largest at the electrolyte region. This result indicates that the thermal stress at the electrolyte region is the most important factor for the decomposition of SOFC. The heat absorbed by hydrogen gas is comparable to that by oxygen gas. The half of heat energy generated in SOFC is transported to the hydrogen gas chamber near the entrance region of the tubular SOFC.

Conclusion

The simulation of the temperature distribution in solid oxide fuel cell was demonstrated. The heat energy produced by the entropy change of electrode reactions was taken into account for the calculation. The calculation under various conditions will give the guideline for the design of solid oxide fuel cell. For the calculation of the temperature distribution in solid oxide fuel cell, the heat produced from the entropy change of electrode reaction will become larger than those by overpotentials and ohmic resistances with the development of the excellent materials and processes.

In this study, the dependencies of thermal and electrochemical parameters on temperature were not taken into account for the calculation of the temperature distribution. However, the deviation from the true temperature distribution in the model cell, which cannot be measured, may not be significant, because the dependencies of parameters on temperature may be negligible small for the temperature distribution in SOFC. The tendency of the temperature distribution calculated in this study might be similar to that of true temperature distribution in the model cell. The calculation under various conditions will provide the useful information for the selection of materials and the construction of SOFC.

This work was supported by the Grant-in-Aid for Scientific Research No. 62603016 from the Ministry of

Education, Science and Culture.

Kyoto University assisted in meeting the publication costs of this article.

References

1) H. S. Isaacs and L. J. Olmer, *J. Electrochem. Soc.*, **129**, 436 (1982).

2) W. Feduska and A. D. Isenberg, *J. Power Sources*, **10**, 89 (1983).

3) Z. Takehara, K. Kanamura, and S. Yoshioka, *J. Electrochem. Soc.*, **136**, 2506 (1989).

4) M. Simoseki and H. Fujinuma, "PC-9801 Finite Element Method/Thermal Stress under Non-Steady State Programing," Nikkan Kogyo Sinbunsha, Tokyo (1989).

5) N. J. Maskalick and D. K. Mclain, *J. Electrochem. Soc.*, **135**, 6 (1988).

6) N. Nakagawa and M. Ishida, *Ind. Eng. Chem. Res.*, **127**, 1181 (1988).

7) E. J. L. Schouler and H. S. Isaacs, *Solid State Ionics*, **5**, 555 (1981).

8) A. E. McHale and H. L. Tuller, *Solid State Ionics*, **5**, 515 (1981).

9) G. Wilemski, *J. Electrochem. Soc.*, **130**, 117 (1983).

10) A. Hirano, S. Nakamura, M. Ippommatsu, and K. Ishimaru, *Denki Kagaku*, **58**, 842 (1990).